

Strain-stress simulation and comparison of different welding sequences during manufacturing of packing vacuum cover

Yanhu Wang¹, Xizhang Chen^{1,2} and Sergey Konovalov^{2,3}

¹ School of Mechanical and Electrical Engineering, Wenzhou University, 276 Xueyuan Middle Rd, Lucheng, Wenzhou 325035, China

² Hualian Machinery Group CO.LTD, Area A China Import and Export Fair Complex, Wenzhou, 325000, China

³ Department of Physics n.a. Prof. V.M. Finkel, Siberian State Industrial University, 42 Kirova Street, Novokuznetsk, 654007, Russia

E-mail: kernel.chen@gmail.com

Abstract. Double ellipsoid heat source model was used to simulate the welding strain-stress evolution during the welding of a vacuum cover for packing machine. Results showed that each welding process has influence about the deformation and residual stress distribution over product. Stress concentration area was found in an area of the cover and the improved structure, manufacturing technologies were proposed to minimize residual stress after simulation and comparison of different manufacturing process, it is an available method to improve the product quality and reduce residual stresses.

1. Introduction

Vacuum cover is one of the most important components for packing machine, its fabrication quality is the key for the working performance. Welding is the main technology used to fabricate the vacuum cover, one of the most challenges is the rupture of the whole cover result from external air pressure. The welding technologies of austenitic stainless steel are well established, but the mechanism of strain-stress formation and distribution are not completely understood yet, especially for those components with complex welding structure and sequences of manufacturing. Austenitic stainless steels have a high thermal expansion coefficient and a lower heat transfer coefficient, which would result in tensile residual stress due thermal gradient from welding process [1]. Residual stress of stainless steel welded joints contributes for stress corrosion cracking. Deformation will also lead to some problems in assembly process, for example, it reduces the mechanical resistance of the structure and seriously affects the quality of welded parts. So, understanding about welding distortion and residual stress for this mechanical component are particularly important [2].

In this paper, SYSWELD software was used to simulate strain-stress evolution during welding fabrication of a vacuum cover. The temperature field distribution, welding deformation and stress were calculated and analyzed, which provides a theoretical basis for the reduction of welding defects and the improvement of product quality.

2. Simulation



2.1. Heat source

There are three common heat source models for hot-working process, i.e. two-dimensional (2D) Gaussian model, double ellipsoid model and three-dimensional (3D) conical Gaussian model. 2D Gaussian model is mainly used for surface heating, such as surface heat treatment. Double ellipsoid model is mainly used for fusion welding. 3D conical Gaussian model is mainly used in some high-energy beam such as laser, plasma and electron beam. It is convenient to calculate by double ellipsoid heat source model, because the TIG welding technology is used. Double ellipsoid heat source model was shown in Figure 1 [3-5].

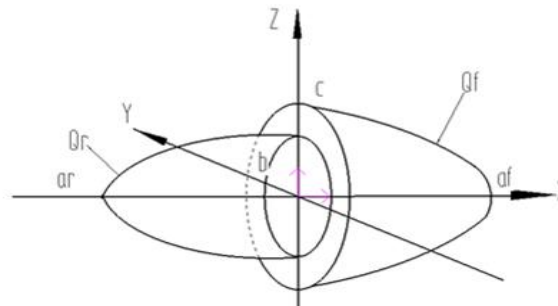


Figure 1. Double ellipsoid heat source model.

Where a_f , a_r , b and c in Figure 1 are the main Gaussian parameters, a_f is the length of the front half ellipsoid, a_r is the length of the rear half ellipsoid, b is the depth of penetration of the $\frac{1}{2}$ and c is the weld width of $\frac{1}{2}$. The welding parameters used are: welding current 380 A, welding voltage 20V, welding speed 5mm/s, melting depth 3 mm, penetration 3 mm, melting width 4 mm and the efficiency 0.7. When the heat source is checked, only a part of the 2D and 3D grids are checked. After repeated correction, the heat source function is determined, save it to a function library for using when the simulation is calculated.

2.2. Model building

A 3D model is built according to the product dimension with the solid works software. Dimensions are shown in Figure 2. The 3D model is shown in Figure 3. Tungsten Inert Gas Welding (TIG) was used in each diagonal seam welding. Since the entire piece is not a ramp, they need two welds on each corner. The number 1 to 8 is weld representative in Figure 3(a) and (b). Figure 3 (a) is the current welding sequence and Figure 3 (b) is the welding sequence after weld adjustment. Welding sequence is in accordance with numbers in the figure.

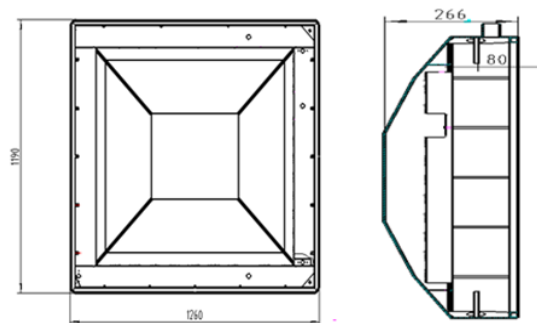


Figure 2. Dimensions of vacuum cover.

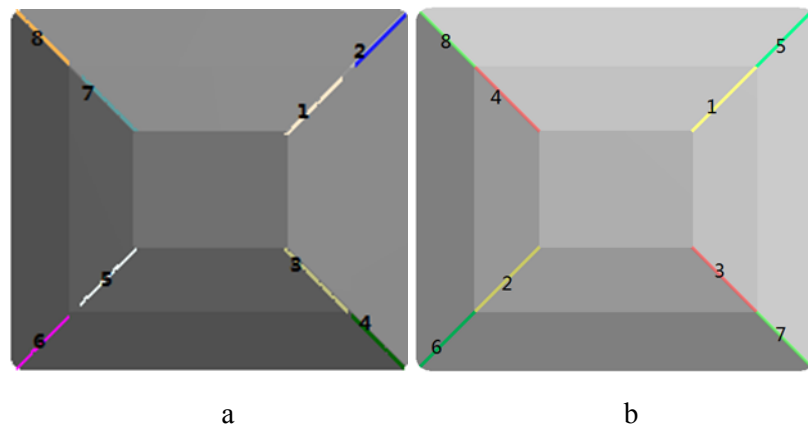


Figure 3. Three-dimensional solid model of vacuum cover (a – current welding sequence; b – welding sequence after weld adjustment).

2.3. Meshing

The complete 3D model is imported into Visual Mesh to mesh. The 3D meshing process is shown in Figure 4. The quality of the grid directly determines the accuracy and efficiency of the calculation. To ensure the accuracy of the premise, the main parts of the grid are denser, the results are not significantly affected by the use of sparse partition. For example, the area away from the weld can choose the larger size of the grid [6]. The mesh elements in the weld seam and the surrounding area are refined. Because of irregular shape, we also use a single area division to ensure the weld area near the surface is totally hexahedral mesh. Area away from the weld, sparse partitioning and a small amount of tetrahedral mesh are allowed. The completed grid is shown in Figure 5. The mesh model contains 54627 units, 38160 nodes, and a total of 77 groups.

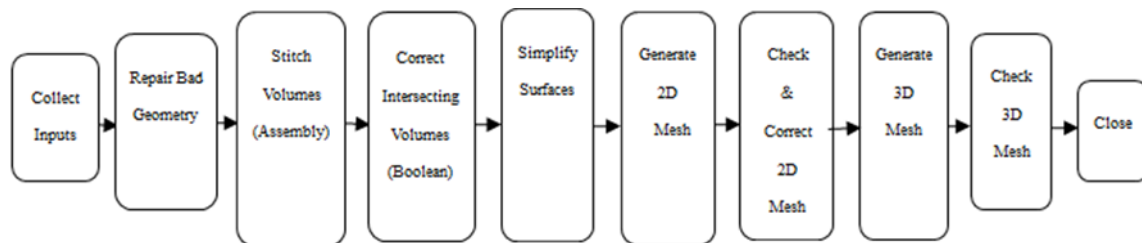


Figure 4. 3D mesh process.

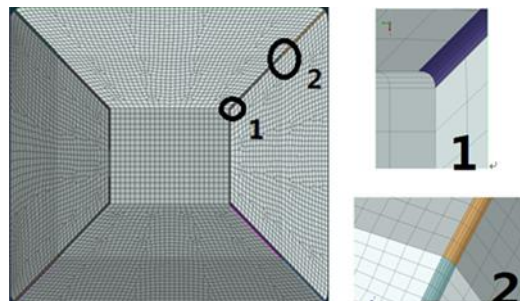


Figure 5. Meshing model (number 1 is the enlarged view of a weld combined with the parts top, number 2 is the enlarged view of a combination of the two welds at the slope).

2.4. Pretreatment and simulation

SYSWELD software was used for simulation. Boundary conditions are required for the calculation of the welding stress and strain field. The main purpose of applying boundary conditions is to prevent the

rigid displacement during calculation and when the results cannot converge. However, the applied boundary conditions can not seriously prevent the free relief of stress and the free deformation during welding. Austenite stainless steel 0Cr18Ni9 is used as base material in the welding of vacuum cover.

There are 8 weld seams as shown in Figure 3 (a) and (b). The simulated welding sequence is the same as the actual works. According to the results of the first weld simulation, the average temperature of the weld heat section is exported as curve Figure 6, the most dramatic change period of temperature is choose as all the other seams' welding heat source.

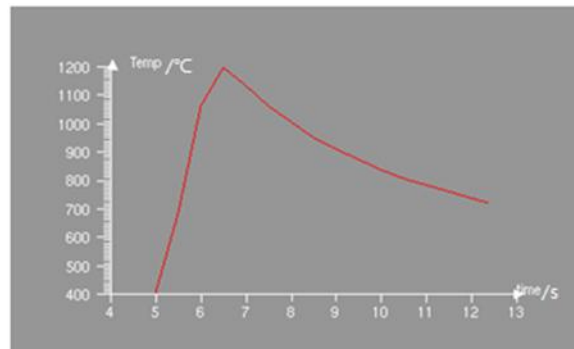
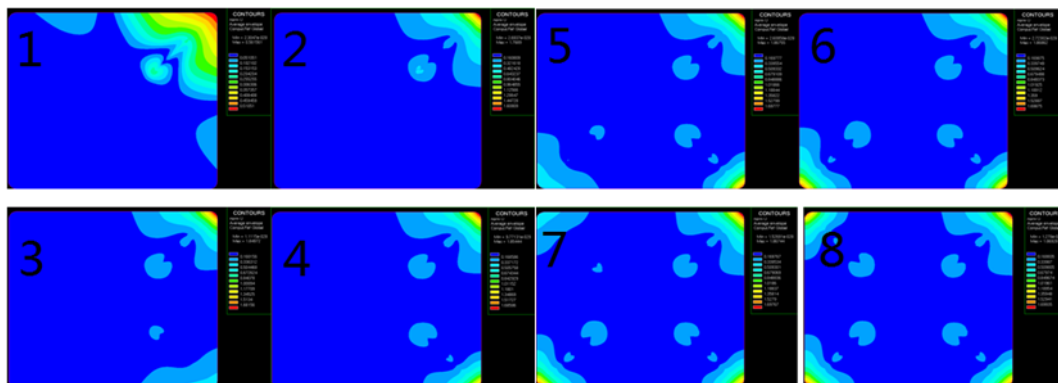


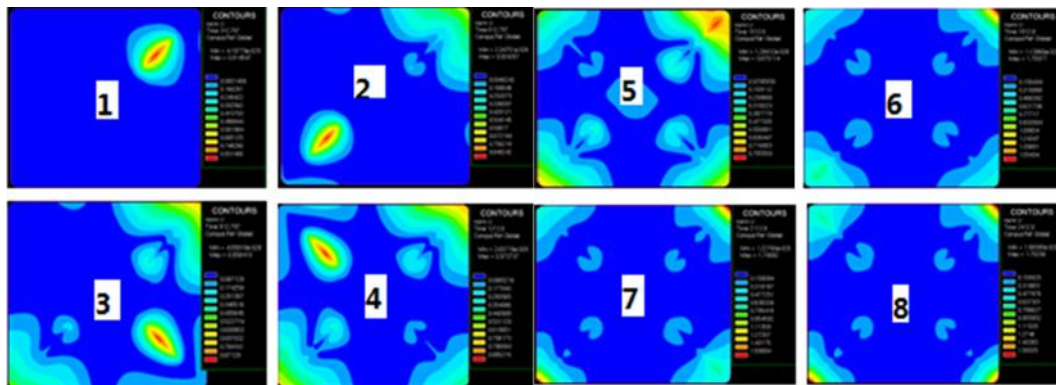
Figure 6. Heat source.

3. Result and analysis

The deformation and stress of each welding stage are shown in Figure 7 and Figure 8, separately. Number 1 to 8 indicates each weld seam sequence. Welding deformation is frequently occurred in production of welding structures. It will not only affect the accuracy and appearance of the welded structure, but also reduce mechanical properties and then result in fracture [7]. According to the size and of the shape of this component, variable simulation results shown in Figure 7 (a) and (b), the maximum strain occurred at the fourth corners, as well as at the beginning of the welding seam. Because of the influence of the first weld seam to the latter one, it caused the amount superposition of the deformation. The deformation increases linearly with the increase of the number of the welding seams. It may be caused by the increasing open groove angle from top to bottom. The groove gaps of the four corners are the largest, where the deformation is greater than other parts. Comparing Figure 7 (a) with (b), we find that at the first welding process, the weld distortion is significantly more than the second welding process corresponding to the deformed position. In the current welding sequence the maximum deformation is 1.699 mm. The maximum amount of deformation of welding sequence after weld adjustment is 1.593 mm. It results in 7% less deformation.



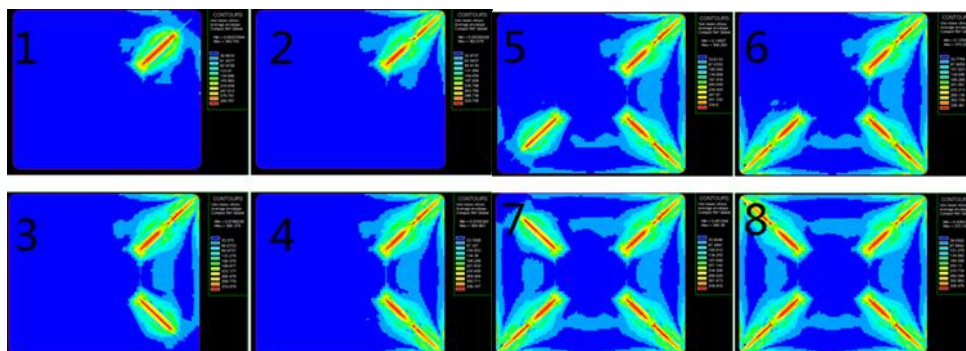
a



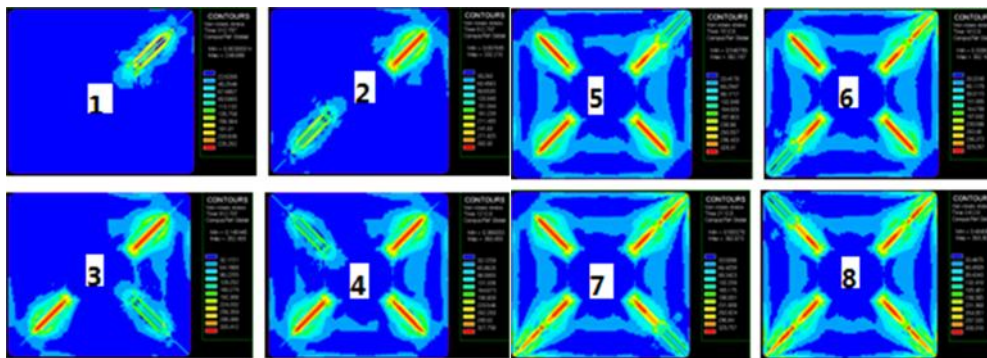
b

Figure 7. Strain cloud image (a – strain cloud image of the current welding sequence; b – strain cloud image of the welding sequence after weld adjustment).

Thermal elastic-plastic analysis, inherent strain method, viscoelastic plastic analysis and coupling effect theory considering the phase transformation and thermal stress are commonly used to study the welding stress and strain. The thermal elastic-plastic analysis method is to calculate the thermal stress and strain in the process of welding thermal cycle [8]. Analysis of thermal elastic-plastic behavior of metallic materials is very complicated. The finite element method can give the deformation history and temperature change of each part of the deformable body in the numerical simulation of the metal welding process. Through stress cloud in Figure 8 (a) and (b), we know the stress at the center of the weld is the largest and therefore each seam center is the stress concentration area. Each weld seam has an effect of welding stress superposition on the next weld. The stress is also correspondingly become larger with the increasing number of the welds. The location of the maximum stress will also change. Comparing stress clouds in Figure 8 (a) and (b), we find weld stress in each seam area is very small, but with the next welding seam the stress increased rapidly, stress amplitude change significantly under the current welding sequence. And, the stress value increases rapidly at each of the weld areas, which is obviously different from the stress distribution obtained after sequence adjustment. The strains after welding sequence adjustment produce less deformation, which would improve the service life of vacuum cover and reduce the possibility of welding defects formation. Generally, the larger weld area stress is, more possible is the defects appear in the weld seam, such as the cracks.

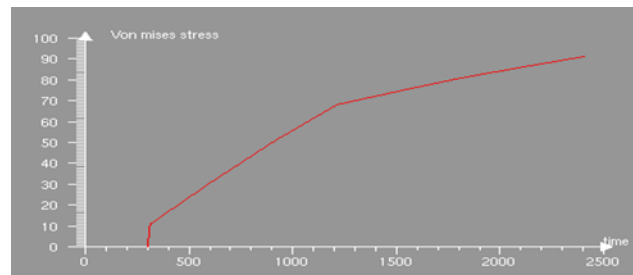


a

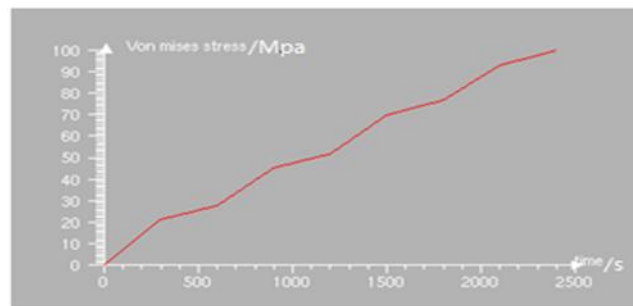


b

Figure 8. Von Mises stress cloud image (a – Von mises stress cloud image of current welding sequence; b – Von Mises stress cloud image of the welding sequence after weld adjustment).



a



b

Figure 9. The average stress curve (a – the average stress curve of current welding sequence; b – the average stress curve of the welding sequence after weld adjustment).

From Figure 9 (a) and (b), we know the average stress of the welding parts is increasing with the increase of the number of welding. But by comparison Figure 9 (a) and (b), for the current welding sequence, the average stress of the work piece at the beginning of the second welds (the first weld end time is 300s) stepwise increases, this change will have a greatly effect on the work-piece, while the welding sequence after weld adjustment, the average stress of the work-piece with the first weld gradually increased. The influence of the welding seam on the welding parts includes the stress and strain distribution, as shown in Table1.

Table1. Simulation result data (current welding sequence; b:welding sequence after weld adjustment)

Number (Weld process types)	Maximum strain (mm)	Maximum stress value (Mpa)	The position of the maximum strain	The distribution position of the maximum stress
1 (a)	0.510	309.767	The 2 th corner weld	The 1 st weld seam
2 (a)	1.608	329.706	The 2 th corner weld	The 1 st weld seam and in 2 nd half before the beginning of the weld
3 (a)	1.681	333.078	The 2 th corner weld	The 1 st and 3 rd weld seam and in 2 nd half before the beginning of the weld
4 (a)	1.685	336.337	The 2 th corner weld	The 1 st and 3 rd weld seam and in 2 nd and 4 th half before the beginning of the weld
5 (a)	1.698	334.800	The 2 th and 4 th corner weld	The 1 st , 3 rd and 5 th weld seam and in 2 nd and 4 th half before the beginning of the weld
6 (a)	1.699	336.381	The 2 th , 4 th and 6 th corner weld	The 1 st , 3 rd and 5 th weld seam and in 2 nd , 4 th and 6 th half before the beginning of the weld
7 (a)	1.698	334.916	The 2 th , 4 th and 6 th corner weld	The 1 st , 3 rd , 5 th and 7 th weld seam and in 2 nd , 4 th and 6 th half before the beginning of the weld
8 (a)	1.700	336.578	The 2 th , 4 th , 6 th and 8 th corner weld	The 1 st , 3 rd , 5 th and 7 th weld seam and in 2 nd , 4 th , 6 th and 8 th half before the beginning of the weld
1 (b)	0.831	248.888	The 1 st weld seam	The 1 st weld seam
2 (b)	0.840	332.216	The 2 nd weld seam and the corners of the 5 th seam weld	The 1 st weld seam but the value increases
3 (b)	0.871	352.439	The 3 rd weld seam and the corners of 5 th seam weld	The 1 st and 2 nd weld seam but the value increases
4 (b)	0.885	360.493	The 4 th weld seam and corners of the 5 th and 6 th seam weld	The 1 st , 2 nd and 3 rd weld seam but the value increases
5 (b)	0.796	362.187	The 5 th weld seam, the	The 1 st , 2 nd , 3 rd and 4 th weld

			corners of the 5 th , 6 th and 7 th seam weld	seam but the value increases
6 (b)	1.554	362.161	The correspond corners of the fifth seam weld	The 1 st , 2 nd , 3 rd , 4 th , 5 th weld seam
7 (b)	1.590	362.673	The corners of the fifth and sixth seam weld	The 1 st , 2 nd , 3 rd , 4 th , 5 th and 6 th weld seam but the value increases
8 (b)	1.593	363.302	The corners of the fifth, sixth and seventh seam weld	The 1 st , 2 nd , 3 rd , 4 th , 5 th , 6 th and 7 th weld seam but the value increases

4. Conclusions

The deformation and residual stress of the welded parts are successfully simulated by using SYSWELD software under two welding process. With the increasing of weld seam numbers, the stress of the welding increases and the maximum stresses are at the intersection of the two welds. Computational simulation results guided us to establish the best welding sequence for structure of the vacuum cover. By comparison with simulated results, we can see that the welding sequence after weld adjustments have reduced deformation and as consequence reduced residual stress in the structure. The results have been used to improve the welding fabrication of vacuum cover of packing machine.

5. Acknowledgements

This work was partly sponsored by National Natural Science Foundation of China (No.51575401), Zhejiang Provincial Natural Science Foundation (No. LY16E050007). We appreciate Mr. Cristiano da Silva Varzim to polish the language and review the paper before submit to publication.

6. References

- [1] Xizhang Chen, Shuyan Zhang, Jingjun Wang and Joe Kelleher F 2015 *Materials and Design* **76** 26–31
- [2] Xizhang Chen, Xing Chen, Huili Xu and Bruce Madigan 2015 *Int. J. Adv. Manuf. Tech.* **80** (5–8) 1197–1211
- [3] Peilin Li and Hao Lu 2011 *Transactions of the China Welding Institution* **11** 66–70
- [4] Jinzhou Zhang 2010 *Journal of Yangtze University* **3** 50–53
- [5] Yu Kang, Yuejin Ma, Wenlin Zhang, Jianguo Zhao and Wei Me 2008 *J. Agric. Univ. Hebei* **2** 36–38
- [6] Amaraeh, Mebanin and Allaloun 2005 *Proc. CAOL 2005 and Int. Conf. on Advanced Optoelectronics and Lasers* (USA: IEEE) 146–154
- [7] Ruiyun Ming 2010 *Welding Technology* **12** 44–46
- [8] Wei Li, Zefeng Wen, Lei Wu and Xuesong Jin 2010 *J. of Mech. Eng.* **46** (10) 95–101